Heat and Mass Transfer of Magneto-Micropolar Fluid Flow Past a Nonlinear Stretching Sheet in a Porous Medium with Chemical Reaction

E. O. Fatunmbi[1], O. O. Akanbi [2]

[1-2]Department of Mathematics and Statistics, Federal Polytechnic, Ilaro, Nigeria.
E-mail: [1] olusojiephesus@yahoo.com; ephesus.fatunmbi@federalpolyilaro.edu.ng;
[2]olumuyiwaaakanbi@yahoo.com

Abstract
The objective of this study is to analyze the flow, heat and mass transfer characteristics of magneto-micropolar chemically reactive fluid over a nonlinear stretching sheet in a saturated non-Darcy porous medium. The impact of viscous dissipation and non-uniform heat source/sink are checked under the influence of prescribed surface temperature and concentration boundary conditions. The model equations governing the problem are reduced from partial to ordinary differential equations using a suitable similarity conversion analysis and then solved via shooting technique with Runge-Kutta algorithms. The numerical outcomes of the simulation are illustrated graphically while a comparison of the present numerical analysis with previous reported data in literature for some limiting situations shows an excellent agreement. The results indicate that the velocity and microrotation profiles advance as the material parameter increases with the motion of micropolar fluid higher than that of Newtonian fluid and that the momentum and thermal boundary layer thicknesses become thin with an increase in the nonlinear stretching parameter.
Keywords: Micropolar fluid; nonlinear stretching sheet; porous medium; chemical reaction.

1 Introduction

1.1 Why Micropolar Fluid?

The Newtonian fluids cannot effectively describe the complex mechanical behaviour that fluid exhibit at micro level. The flow of most fluids of industrial and engineering applications cannot be accurately explained by the Navier-Stokes equations of classical hydrodynamic as these fluids are non-Newtonian. Various development of various microcontinuum theories have been done such as the simple microfluids, simple deformable directed fluids, polar fluids, anisotropic fluids and micropolar fluids depending on diverse physical characteristics.

Moreso, due to diverse fluid characteristics in nature, different models of non-Newtonian fluids have been formulated, for instance, thed Casson fluid, Jeffery fluid, Maxwell fluid, Ostwald de-Waele power law fluid and Micropolar fluids (Chen *et al.*, 2011). Micropolar fluid is prominent among others because it offers a good mathematical model for simulating the flow characteristics of polymeric suspensions, colloidal fluids, liquid crystals, animal blood etc.

The theory of micropolar fluids formulated by Eringen (1966) which was later and extended to include the concept of thermo-micro polar fluids by Eringen (1972). It has since attracted the interest of researchers and scientist in the recent years. This is because it provides a good mathematical framework for simulating the flow characteristics of real and important fluids including the flow of blood, biological fluids, polymeric additives, colloidal suspensions, liquid crystals and so on. Micropolar fluid is prominent among the non-Newtonian fluids. The concept of micropolar fluid deals with a class of fluids that exhibit certain microscopic effect arising from the local structure and micromotion of the fluid element. These are fluids with microstructure which constitutes a substantial generalization of the Navier-Stokes model that open up a new field of potential applications. Such fluids are of a complex nature and individual fluid particles may be of different shapes and may shrink and/or expand, occasionally changing shapes and rotating independently of the rotational movement of the fluid (Lukaszewicz, 1999; Rana and Reena, 2009 Ahmadi, 1976; Peddieson, 1972).

Stretching sheet flow was pioneered by Sakiadis (1961). Crane (1970) also improve on such study. Various applications of heat and mass transfer over stretching surfaces in industrial and engineering processes include: extrusion of plastic sheet and metal extrusion, hot rolling, paper and textile production. Similarly, convective transport phenomena in porous media is applicable in the engineering operations as in crude oil extraction; ground water hydrology, underground disposal of waste, biomedical engineering; spreading of chemical pollutants in saturated soil (Ramya *et al.*, 2018; Akinbobola and Okoya, 2015; Cortell, 2007).

The importance of chemical reaction and radiation effect can be found useful in the design of chemical processing equipment and combustion processes, temperature and moisture distribution over agricultural fields, food processing, nuclear power plant, steel rolling, electric power generation etc (Fatunmbi and Fenuga, 2017; Ibrahim and Suneetha, 2014; Ibrahim, 2014).

This study is therefore aims at investigating the heat and mass transfer of MHD micropolar fluid over a stretching with the influence of radiation, chemical reaction as well as porous medium under the influence of surface mass flux. By means of relevant similarity conversion analysis, the modelled equations have been translated from partial to ordinary differential equations and then integrated numerically via fourth-order Runge-Kutta method.

2 Formulation and Development of the Problem

The following assumptions have been put in place for the formulation of the governing equation modelling the problem

- The flow is two-dimensional (x, y), incompressible and steady.
- The sheet is permeable and stretching nonlinearly with velocity $u_w = cx^r$.
- The corresponding velocity components are (u, v).
- x axis is taken along the direction of flow with y axis normal to it.
- The fluid is electrically conducting Micropolar fluid.
- Applied magnetic field is normal to the flow direction.
- The induced magnetic field is sufficiently small and negligible and no electric field.
- The surface mass flux is assumed to be a function of x.
- Non-uniform heat source/sink is applied with viscous dissipation effect.
- A chemical species diffuses into the ambient fluid initiating an irreversible homogeneous first order chemical reaction.

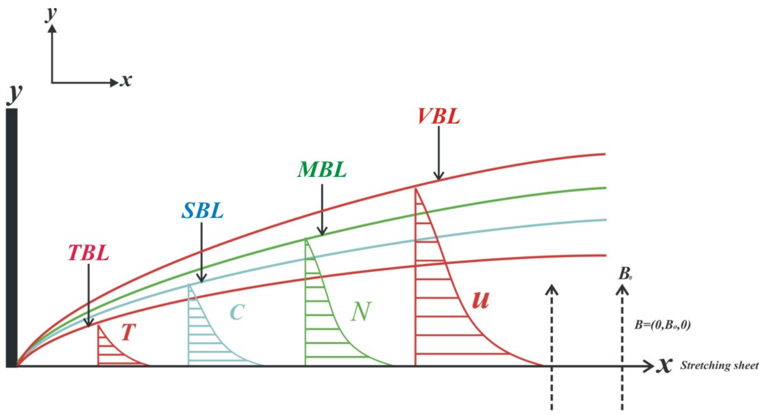

Figure 1: Flow Configuration and the Coordinate System.

2.1 The Governing Equations

Continuity Equation

$$\frac{\partial u}{\partial x} + \frac{\partial v}{\partial y} = 0, \tag{1}$$

Momentum Equation

$$u\frac{\partial u}{\partial x} + v\frac{\partial u}{\partial y} = \frac{(\mu+\mu_r)}{\rho}\frac{\partial^2 u}{\partial y^2} + \frac{\mu_r}{\rho}\frac{\partial N}{\partial y} - \frac{\sigma B^2(x)}{\rho}u - \frac{\nu}{K_p}u - \frac{F}{K_p}u^2, \tag{2}$$

Microrotation Equation

$$u\frac{\partial N}{\partial x} + v\frac{\partial N}{\partial y} = \frac{\gamma}{\rho j}\frac{\partial^2 N}{\partial y^2} - \frac{\mu_r}{\rho j}\left(2N + \frac{\partial u}{\partial y}\right), \tag{3}$$

Energy Equation

$$u\frac{\partial T}{\partial x} + v\frac{\partial T}{\partial y} = \frac{k}{\rho C_p}\frac{\partial^2 T}{\partial y^2} + \frac{(\mu+\mu_r)}{\rho C_p}\left(\frac{\partial u}{\partial y}\right)^2 + \frac{\sigma B^2(x)}{\rho C_p}u^2 + \frac{q'''}{\rho C_p}, \tag{4}$$

Concentration Equation

$$u\frac{\partial C}{\partial x} + v\frac{\partial C}{\partial y} = Dm\frac{\partial^2 C}{\partial y^2} - k_c\left(C - C_\infty\right). \tag{5}$$

The Boundary Conditions

$$u = u_w = cx^r, v = v_w, N = -h\frac{\partial u}{\partial y}, T = T_w = \left(Ax^n + T_\infty\right), C = C_w = \left(Bx^m + C_\infty\right) \quad at\ y = 0,$$
$$u \longrightarrow 0, N \longrightarrow 0, T \longrightarrow T_\infty, C \longrightarrow C_\infty \quad \text{as} \quad y \to \infty. \tag{6}$$

The Non-uniform heat source/sink q''’

$$q''' = \frac{\kappa u_w}{x^r \nu}\left[A^\star\left(T_w - T_\infty\right)f' + B^\star\left(T - T_\infty\right)\right] \tag{7}$$

The Suction Velocity and the applied magnetic field varies in strength such that (see Makinde, 2011; Yazdi *et al.*, 2011)

$$V_w = V_0 x^{(r-1)/2}, B(x) = B_0 x^{(r-1)/2} \tag{8}$$

where V_0 and B_0 are also a constants. The various symbols used in the governing equations are described in Table 1.

Table 1: Description of the symbols used

Symbols	Nomenclature	Symbols	Nomenclature
μ	dynamic viscosity	ρ	density
μ_r	vortex viscosity	ν	kinematic viscosity
σ	electrical conductivity	T	fluid temperature
n	surface Temp. Parameter	C	fluid concentration
m	surface Conc. Parameter	Dm	mass diffusivity
k^*	mean absorption coefficient	$\sigma^\star$	Stefan-Boltzmann constant
u	velocity component in x	h	surface parameter
v	velocity component in y	$A\&B$	constants
γ	spin gradient viscosity	V_w	suction/injection term
k	thermal conductivity	k_c	rate of chemical reaction
N	microrotation component	A^*	space dependent heat source

3 Methodology

3.1 The Transformation Variables

(see Hayat *et al.*, 2008; Salem, 2013; Waqas *et al.*, 2016)

$$\begin{aligned}
&\eta = y\left[\frac{c(r+1)x^r}{2x\nu}\right]^{1/2},\ N = x^{(3r-1)/2}\left[\frac{c^3(r+1)}{2\nu}\right]^{1/2} g(\eta),\ u = cx^r f', \\
&v = -\left[\frac{c\nu(r+1)}{2}\right]^{1/2} x^{(r-1)/2}\left(f + \frac{(r-1)}{(r+1)}\eta f'\right),\ \gamma = \left(\mu + \frac{\mu_r}{2}\right) j, \\
&\theta(\eta) = \frac{T - T_\infty}{T_w - T_\infty},\ \phi(\eta) = \frac{C - C_\infty}{C_w - C_\infty}.
\end{aligned} \tag{9}$$

3.2 The Transformed Equations

Substituting (9) into the governing equations (2-6) gives

$$(1+K)\,f''' + ff'' + Kg' - 2\left(\frac{r+Fs}{r+1}\right)f'^2 - \left(\frac{2}{r+1}\right)(M+Da)f' = 0, \tag{10}$$

$$(1+K/2)\,g'' + fg' - \left(\frac{3r-1}{r+1}\right)f'g - K\,(2g+f'')\left(\frac{2}{r+1}\right) = 0, \tag{11}$$

$$\begin{aligned}
&\theta'' + Pr\left(f\theta' - \frac{4n}{r+1}f'\theta\right) + (1+K)\,PrEcf''^2 + \left(\frac{2}{r+1}\right)PrMEcf'^2 + \\
&\left(\frac{2}{r+1}\right)Pr\,(\alpha f' + \beta\theta) = 0.
\end{aligned} \tag{12}$$

$$\phi'' + Scf\phi' - \left(\frac{2m}{r+1}\right)Sc\phi f' - \left(\frac{2}{r+1}\right)Sc\zeta\phi = 0, \tag{13}$$

The boundary conditions are:

$$\begin{aligned}
&\eta = 0 : f' = 1,\ f = fw,\ g = -hf'',\ \theta = 1, \phi = 1 \\
&\eta \longrightarrow \infty : f' = 0,\ g \longrightarrow 0,\ \theta \longrightarrow 0, \phi \longrightarrow 0.
\end{aligned} \tag{14}$$

3.3 The Quantities of Engineering Interest

$$C_{fx} = \frac{\tau_w}{\rho u_w^2},\ Nu_x = \frac{xq_w}{\kappa\left(T_w - T_\infty\right)},\ Sh_x = \frac{xq_m}{Dm\left(C_w - C_\infty\right)}, \tag{15}$$

with

$$\begin{aligned} \tau_w &= \left[(\mu+\mu_r)\frac{\partial u}{\partial y} + \mu_r N\right]_{y=0},\ q_w = -\left(\kappa\frac{\partial T}{\partial y}\right)_{y=0}, \\ q_m &= -\left(Dm\frac{\partial C}{\partial y}\right)_{y=0} \end{aligned} \tag{16}$$

The dimensionless skin friction coefficient is

$$C_{fx} = \left(\frac{r+1}{2}\right)^{1/2}\left[1 + (1-h)\,K\right] Re_x^{-1/2} f''(0), \tag{17}$$

while the Nusselt and Sherwood numbers respectively simplify to

$$Nu_x = -\left(\frac{r+1}{2}\right)^{1/2} Re_x^{1/2}\theta'(0),\ Sh_x = -\left(\frac{r+1}{2}\right)^{1/2} Re_x^{1/2}\phi'(0). \tag{18}$$

4 Result Analysis and Discussion

The current study has been solved numerically due to the highly nonlinearity of the involving governing equations. The shooting technique has been employed alongside the Runge-kutta order four using Maple 2016. The validity of the numerical code has been checked by direct comparison of the computational values gotten in this study with earlier reported related studies in literature in the limiting cases. The values of the skin friction coefficient C_{fx} and the Nusselt numbers Nu_x have been found directly from the numeric.

4.1 Comparison of The Present Results with Existing Work

The present work has been compared with the related published works in the literature in order to ascertain the accuracy and validity of the numerical code employed in the solution. The works of those authors compared with are special cases of the present study. Table 2 clearly reveals that there exists a good relationship between the computational values of the skin friction coefficient C_{fx} of Kumar (2009) and Hayat *et al.*, (2008) for changes in K with the current study.

Table 2: Comparison of values of the skin friction coefficient C_{fx} with existing results

K	Kumar (2009)	Present	r	Hayat et al. (2008)	Present
0.0	1.000008	1.00000837	00	0.627555	0.627555
1.0	1.367996	1.36799627	0.2	0.766837	0.766837
2.0	1.621575	1.62157505	0.5	0.889544	0.889544
3.0	1.827392	1.82738216	1.0	1.000000	1.000008
4.0	2.005420	2.00542027	1.5	1.061601	1.061601
			3.0	1.148593	1.148593
			7.0	1.216850	1.216850
			10.0	1.234875	1.234875
			20.0	1.257424	1.257424
			100.0	1.276774	1.276774

Similarly, it is evident in Table 3 that a strong correlation exists between the computational values of the Nusselt number Nux of Grubka and Bobba (1985) as well as Chen (1998) for variation in Pr with the present study.

Table 3: Comparison of values of heat transfer rates Nu_x for changes in Pr when $K = \lambda = Ec = M = G_2 = \alpha = \beta = fw = 0$ and $r = 1$

Pr	Grubka & Bobba (1985)	Chen (1998)	Present
0.01	0.0294	0.02942	0.12036573
0.72	1.0885	1.08853	1.08862246
1.0	1.3333	1.33334	1.33333334
3.0	2.5097	2.50972	2.50972158
10.0	4.7969	4.79686	4.79687061
100.0	15.712	15.7118	15.71196466

4.2 Graphs and Discussion

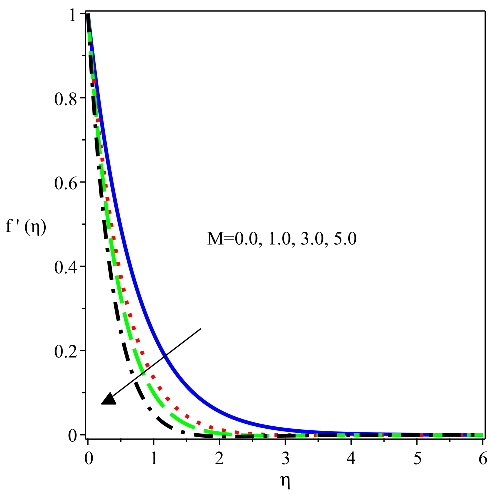

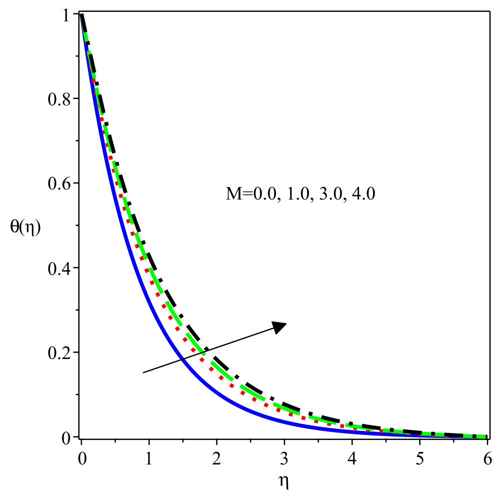

Fig. 2 Velocity. profiles for M **Fig.3**. Temp. profiles for M

From figures 2 velocity decreases while temperature increases with growing values of the magnetic field parameter M. The boundary layer thickness is thinner in case of Velocity due to Lorentz force.

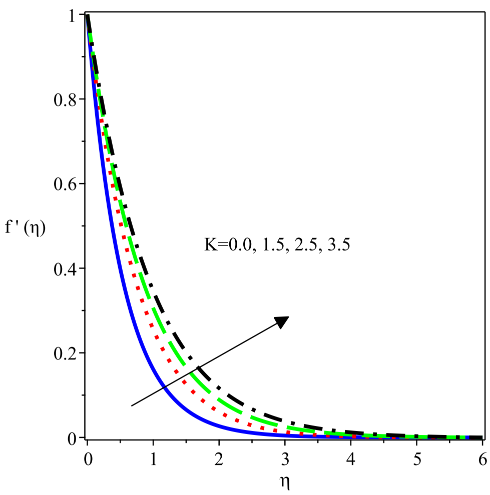

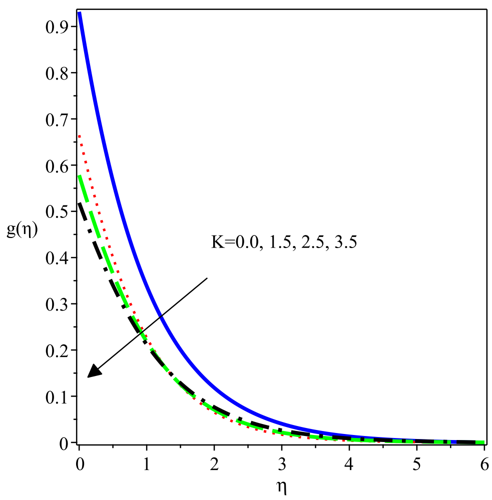

Fig.4. Velocity profiles for K **Fig.5**. Microrotation. profiles for K

The plot in figure 4 shows that the velocity profile increases with a rise in K while micro-rotation distribution decreases with a rise in K. More so, The boundary layer thickness is thinner in case of microrotation profiles.

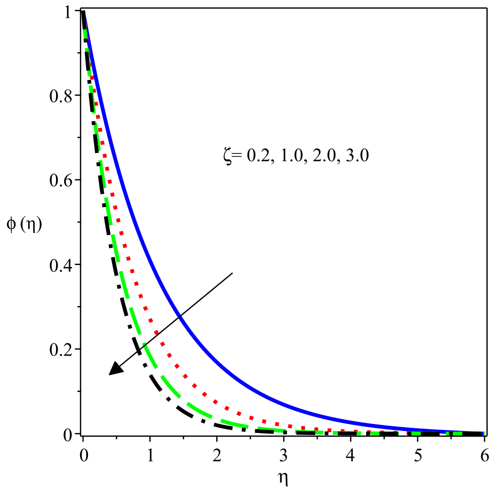

Fig. 6. Concentration. profiles for ζ

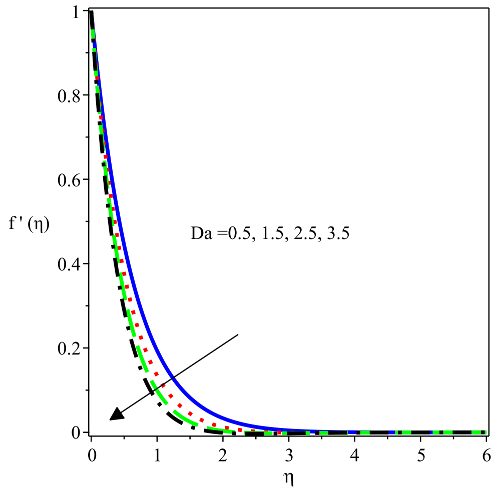

Fig. 7 Velocity. profiles for Da

It is displayed in figure 6 that the concentration field decreases for a rise in chemical reaction parameter ζ. In a similar manner, fluid motion decreases with a rise in Da parameter as depicted in figure 7.

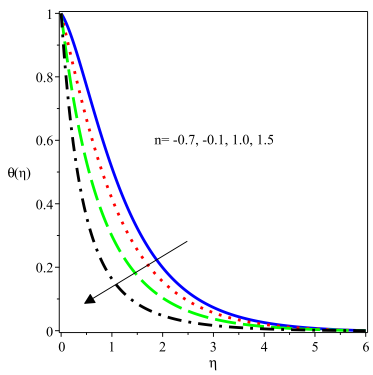

Fig.8. Temperature profiles for n

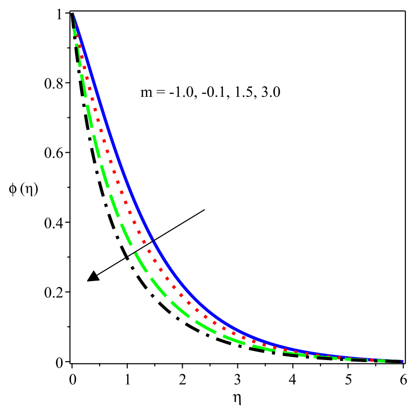

Fig. 9. Concentration profiles for m

Figures 8 & 9 show the effects n and m on Temperature and Concentration profiles. Evidently, the temperature profiles fall for a rise in n while a rise in m also lowers the concentration profiles,

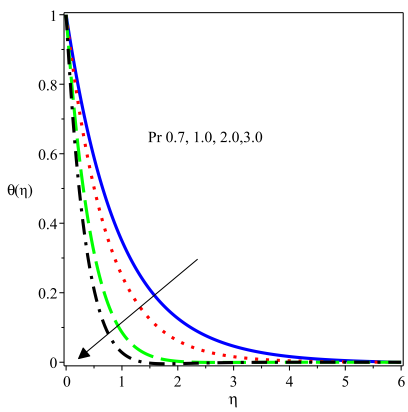

Fig.10. Temperature profiles for Pr

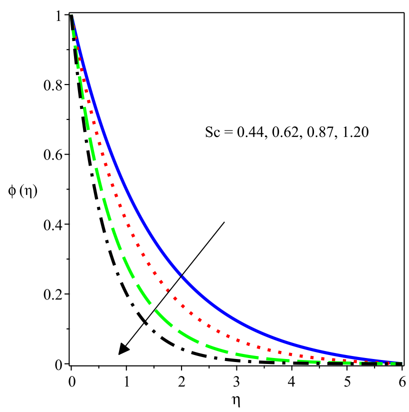

Fig. 11 Concentration profiles for Sc

Figures 10 & 11 show the of effects Pr and Sc on the profile of temperature and concentration profiles respectively. It clearly seen that the temperature distribution falls with a rise in Pr and in the like manner, the concentration field also decreases with growing values of Sc

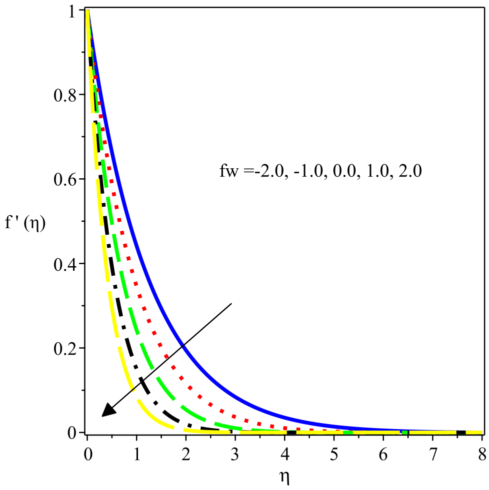

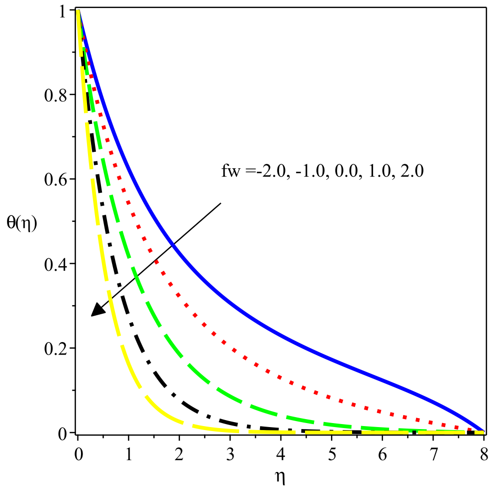

Fig.12. Temp.profiles for Pr **Fig. 13** Conc.profiles for Sc

Figures 12 & 13 describe the effects of fw on velocity and temperature profiles. Both momentum boundary layer and thermal boundary layer thin out for an increase in $fw > 0$. In consequence, the fluid motion and energy distribution decline for a rise in $fw > 0$. This trend is however, reversed with a rise with a rise in $fw < 0$

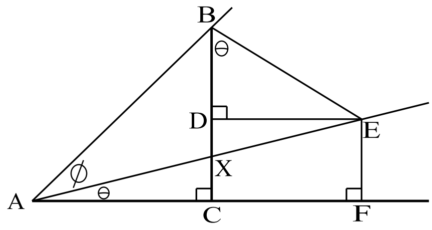

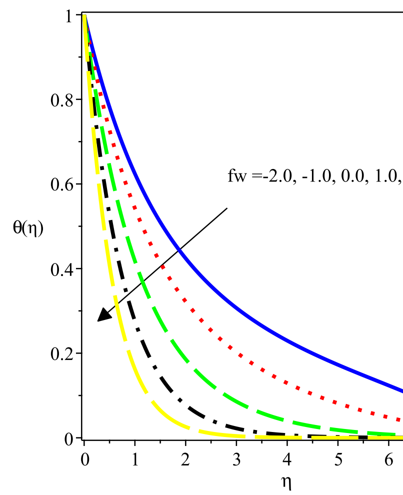

Fig.12. Temp.profiles for Pr **Fig. 13** Conc.profiles for Sc

5 Conclusion

This study has reported heat and mass transfer analysis of magneto-micropolar fluid flow passing a nonlinear stretching sheet in a porous medium with chemical reaction impact. The influence of nonuniform heat source/sink, viscous dissipation are also incorporated. The main equations are translated into dimensionless form via similarity conversion analysis. The resulting equations are computationally solved via shooting techniques and Runge-Kutta algorithm while the results are validated with relevant works in the literature in the limiting cases and found to be in good relationship. From this study, it has been noted that

- The (Cf_x) is found to increase with a rise in r
- Heat transfer rate Nu_x increases for a rise in Pr
- The temperature falls with a rise in the wall surface temperature parameter n.

- The concentration falls with a rise in the wall surface concentration parameter m.
- Injection increases the $f'(\eta)$ while suction lowers it.
- Temperature decreases for an increase in n, Pr and fw.
- Velocity as rises with an increase in K while it falss for M, Da and fw.
- Concentration reduces with a rise in ζ and Sc.
- The BLT is thinner in case of suction than injection in both profiles.

References

Ahmadi, G. (1976). Self-similar solution of incompressible micropolar boundary layer flow over a semi-infinite plate. *Int. J. Engng. Sci, 14*, 639-646.

Akinbobola, T. E. and Okoya, S. S. (2015). The flow of second grade fluid over a stretching sheet with variable thermal conductivity and viscosity in the presence of heat source/sink. *Journal of Nigeria Mathematical Society, 34*, 331-345.

Chen, C. H. (1998). Laminar mixed convection adjacent to vertical continuously stretching sheets. *Heat and Mass Transfer, 33*, 471-476.

Chen, J., Liang, C. and Lee J. D. (2011). Theory and simulation of micropolar fluid dynamics. *J. Nanoengineering and nanosystems, 224*, 31-39. ions, 38, 480-496.

Cortell, R, (2007). viscous flow and heat transfer over a nonlinearly stretching sheet, *Applied Mathematics and Computation 184*, 864–873.

Crane, L. J. (1970). Flow past a stretching plate. *Communicatios Breves, 21*, 645-647.

Eringen, A. C. (1964). Simple microfluids. International Journal of Engineering Science, 2(2), 205-217.

Eringen, A. C. (1966). Theory of micropolar fluids. *J. Math. Anal. Appl., 16*, 1-18.

Eringen, A. C. (1972). Theory of thermo-microfluids. *Journal of Mathematical Analysis and Applications, 38*, 480-496.

Fatunmbi, E. O. and Fenuga, O. J. (2017). MHD micropolar fluid flow over a permeable stretching sheet in the presence of variable viscosity and thermal conductivity with Soret and Dufour effects. *International Journal of Mathematical Analysis and Optimization: Theory and Applications, 2017*, 211- 232.

Das, S., Jana, R. N. and Makinde, O. D. (2015). Magnetohydrodynamic mixed convective slip flow over an inclined porous plate with viscous dissipation and Joule heating. *Alexandria Engineering Journal, 54*, 251-261.

Das, K. and Jana, S. and Kundu, P.K. (2015), Thermophoretic MHD Slip Flow over a permeable surface with variable fluid properties. *Alexandria Engineering Journal*, 35-44.

Grubka, L. J. and Bobba, K. M. (1985). Heat transfer characteristic of a continuous stretching surface with variable temperature, *Journal of Heat Transfer*, 107, 248-250.

Hayat, T. and Abbas, Z. and Javed, T. (2008), Mixed convection flow of a micropolar fluid over a non-linearly stretching sheet. *Physic Letter A*, 372, 637-647.

Ibrahim, S. M. (2014). Effects of chemical reaction on dissipative radiative MHD flow through a porous medium over a nonisothermal stretching sheet. *Journal of Industrial Mathematics, 2014*, 1-10. doi.org/10.1155/2014/243148

Ibrahim, S. M. and Suneetha, K. (2014). Radiation and heat generation effects on steady MHD flow near a stagnation point on a linear stretching sheet in porous medium in presence of variable thermal conductivity and mass transfer. *Int. J. Curr. Res. Aca. Rev., 2*(7), 89-100.

Kumar, L. (2009). Finite element analysis of combined heat and mass transfer in hydromagnetic micropolar flow along a stretching sheet. *Comput Mater Sci, 46*, 841-848. Doi: 10.1371/journal.pone.0059393

Mahmoud, M. A. A. (2012). Thermal radiation effects on MHD flow of a micropolar fluid over a stretching surface with variable thermal conductivity *Physica A , 375*, 401-410. doi:10.1016/j.physa.2006.09.010.

Makinde, O. D. (2011). Second law analysis for variable viscosity hydromagnetic boundary layer flow with thermal radiation and Newtonian heating, *Entropy*, 13, 1446-1464.

Peddieson, J. (1972). An application of the micropolar model to the calculation of a turbulent shear flow. *Int. J. Eng. Sci., 10*, 23-32.

Rahman, M.M and Uddin, M.J. and Aziz, A. (2009). Effects of variable electric conductivity and non-uniform heat source (or sink) on convective micropolar fluid flow along an inclined flat plate with surface heat flux. *International Journal of Thermal Sciences* 48, 2331 - 2340.

Ramya, D., Chamkha, A. J., Srinivasa R. and Rao, J. A. (2018). Effects of velocity and thermal wall slip on magnetohydrodynamics (MHD) boundary layer viscous flow and heat transfer of anano fluid over a non-linearly-stretching sheet:a numerical study, *Propulsion and Power Research*, doi.org/10.1016/j.jppr.2018.04.003

Reena and Rana, U. S. (2009). Effect of Dust Particles on rotating micropolar fluid heated from below saturating a porous medium. *Applications and Applied Mathematics: An International Journal. 4*, 189-217.

Sakiadis, B. C. (1961). Boundary layer behaviour on continuous solid surfaces: II The boundary layer on a continuous flat surface. *A.I.Ch.E.J. 7*, 221-225.

Salem, A.M. (2013), The Effects of Variable Viscosity, Viscous Dissipation and Chemical Reaction and Heat and Mass Transfer of Flow of MHD Micropolar Fluid along a Permeable Stretching Sheet in a Non-Darcian Porous Medium. *Mathematical Problems in Engineering*, 2013,1-10. doi.org/10.1155/2013/185074.

Waqas, M. and Farooq, M. and Khan, M.J. and Alsaedi, A. and Hayat, T. and Yasmeen, T. (2016), Magnetohydrodynamic (MHD) Mixed Convection Flow of Micropolar Liquid Due to Nonlinear Stretched Sheet with Convective Condition, *International Journal of Heat and Mass Transfer,* 102, 766-772.

Yazdi, M. H., Abdulaah, S., Hashim, I. and Sopian, K. (2011). Effects of viscous dissipation on the slip MHD flow and heat transfer past aa permeable surface with convective boundary conditions, *Energies*, 4, 2273-2294.